J. Braz. Chem. Soc., Vol. 20, No. 4, 728-736, 2009.
Printed in Brazil - ©2009 Sociedade Brasileira de Química
0103 - 5053 $6.00+0.00

20 years

Article

Electronic Conduction and Electrocatalysis by Supramolecular Tetraruthenated Copper Porphyrazine Films

Marcio Y. Matsumoto, Marcos M. Toyama, Ildemar Mayer, Herbert Winnischofer, Koiti Araki and Henrique E. Toma*

Instituto de Química, Universidade de São Paulo, CP 26077, 05513-970 São Paulo-SP, Brazil

Uma nova espécie cobre(II)-tetra(3,4-piridil)porfirazina tetrarrutenada, $[CuTRPyPz]^{4+}$ foi sintetizada e sua caracterização conduzida por meio de métodos analíticos, espectroscópicos e eletroquímicos. Sua extensa conjugação-π a distingue dos derivados análogos da *meso*-tetrapiridilporfirina, levando à ocorrência de interações eletrônicas mais fortes entre os complexos periféricos e o anel porfirazínico central. Com base nas interações eletrostáticas e de empilhamento-π, foram realizadas montagens, camada-por-camada, de filmes funcionais, combinando-se a $[CuTRPyPz]^{4+}$ com a ftalocianina de cobre(II) tetrassulfonada, $[CuTSPc]^{4-}$. As propriedades condutoras e eletrocatalíticas desses filmes foram investigadas através de técnicas de impedância e de voltametria de disco rotatório, observando-se um comportamento metálico nas proximidades do potencial do par redox Ru(III)/(II), bem como uma pronunciada atividade catalítica na oxidação de íons nitrito e sulfito, em meio aquoso.

A new tetraruthenated copper(II)-tetra(3,4-pyridyl)porphyrazine species, $[CuTRPyPz]^{4+}$, has been synthesized and fully characterized by means of analytical, spectroscopic and electrochemical techniques. This π-conjugated system contrasts with the related *meso*-tetrapyridylporphyrins by exhibiting strong electronic interaction between the coordinated peripheral complexes and the central ring. Based on favorable π-stacking and electrostatic interactions, layer-by-layer assembled films were successfully generated from the appropriate combination of $[CuTRPyPz]^{4+}$ with copper(II)-tetrasulfonated phtalocyanine, $[CuTSPc]^{4-}$. Their conducting and electrocatalytic properties were investigated by means of impedance spectroscopy and rotating disc voltammetry, exhibiting metallic behavior near the Ru(III/II) redox potential, as well as enhanced catalytic activity for the oxidation of nitrite and sulphite ions.

Keywords: molecular conductors, porphyrazines, ruthenium polypyridines, thin films, electrocatalysis

Introduction

Phthalocyanines and porphyrins are important macrocyclic compounds exhibiting a wide variety of applications in science and technology.[1-13] Their main characteristics are associated with the π-conjugated ring which imparts interesting physical and chemical properties, including the facility of stacking and yielding molecular films. The possibility of rationally manipulating their properties at the nanoscale is a relevant issue to be pursued, aiming the generation of functional molecular materials for nanotechnology devices.[14-17]

As a matter of fact, tetrapyridyl porphyrins have already been modified with transition metal complexes in order to generate convenient building-blocks and connectors for assembling supramolecular systems and nanostructured materials.[18,19] In such systems, the transition metal complexes can play many roles, because of their wide variety of structural, electronic, redox and catalytic properties.[20-26] In particular, the coordination of ruthenium complexes to *meso*-pyridylporphyrins has provided rather versatile systems, in which the chemical and photochemical reactivity can be modulated by the electronic, structural and steric effects induced by the peripheral complexes.[27-32] However, it should be noticed that in the case of tetrapyridyl porphyrins, the electronic coupling between the porphyrin center and the ruthenium complexes is mediated by a

*e-mail: henetoma@iq.usp.br

non-coplanar pyridine bridge, reducing to a great extent, their mutual influence in terms of chemical and physical properties. However, a stronger electronic coupling can be expected for coplanar bridged systems such as the tetra(3,4-pyridyl)porphyrazines. In this case, in contrast to the tetrapyridylporphyrins, the bridging pyridyl rings are fused to the macrocycle, becoming part of the π-extended system.[33-35]

In a previous work,[34] we have demonstrated that the free-base tetra(3,4-pyridyl)porphyrazine molecule can bind four $[Ru(bpy)_2Cl]^+$ complexes, yielding a stable cationic system. Now, we are focusing on a new tetraruthenated copper(II) tetra(3,4-pyridyl)porphyrazine complex, including an investigation on its interaction with the anionic tetrasulfonated copper(II) phtalocyanine species (Figure 1). It should be noticed that while the preparation of the free-base tetra(3,4-pyridyl)porphyrazine species requires rather complicated synthetic procedures to be accomplished,[34] the copper(II) derivative is commercially available and provides a more convenient starting material for expanding the investigation on this series of complexes. So, initially, the $[CuTRPyPz]^{4+}$ complex was synthesized and fully characterized by electrospray ionization mass spectrometry (ESI-MS), UV-Vis spectroelectrochemistry and cyclic voltammetry. Then, layer-by-layer films were electrostatically assembled, and their electrocatalytic activity for nitrite and sulphite oxidation evaluated.

Experimental

Materials

The *cis*-dichloro-*bis*(2,2'-bipyridine)ruthenium(II) complex, $[Ru(bpy)_2Cl_2]$, was prepared by refluxing $RuCl_3 \cdot nH_2O$, LiCl and 2,2'-bipyridine as previously described.[34] Copper(II) tetra(3,4-pyridyl)porphyrazine, and copper(II) phtalocyanine tetrasulfonic acid tetrasodium salt was purchased from Aldrich Chemical Co. and used without purification.

The $[CuTRPyPz]^{4+}$ species was synthesized by refluxing CuTPyPz (100 mg, 0.172 mmol) and $[Ru(bpy)_2Cl_2]$ (372 mg, 0.741 mmol) in trifluoroethanol for 3 h, under an argon atmosphere. After removing the solvent in a flash evaporator, the resulting solid was dissolved in methanol and refluxed again for 3 h. The mixture was filtered and the solvent removed in a rotary evaporator. The solid was washed with acetone and dissolved in a minimum amount of methanol. After adding solid lithium trifluoromethanesulfonate (LiTFMS), the product was precipitated as TFMS salt by adding small amounts of water. Purification was carried out by column chromatography in neutral alumina, starting with a mixture of dichloromethane/ethanol (95:5) and increasing the polarity by the addition of ethanol. Elemental analysis for $Ru_4C_{112}H_{76}N_{28}O_{12}S_4F_{12}Cl_4Cu \cdot 5H_2O$ (3062 g mol^{-1}): Exp. (Calc.) C: 43.62 (43.93); H: 2.91 (2.83); N: 12.97 (12.81).

Layer-by-layer electrostatically assembled films were prepared by transferring a precise volume of a methanol solution of [CuTRPyPz]TFMS onto the electrode surface and allowing it to dry in air. After depositing the first layer of the tetracationic species, the electrode was dipped into a $[CuTSPc]^{4-}$ aqueous solution in order to assemble a bilayered film.[36] After washing with deionized water, the procedure was repeated, alternating the $[CuTRPyPz]^{4+}$ and $[CuTSPc]^{4-}$ solutions for generating multilayered films in a controlled way.

Instrumentation

UV-Vis spectra were recorded on a HP-8453A diode-array spectrophotometer, in the 190 to 1100 nm range. Cyclic voltammetry was carried out in

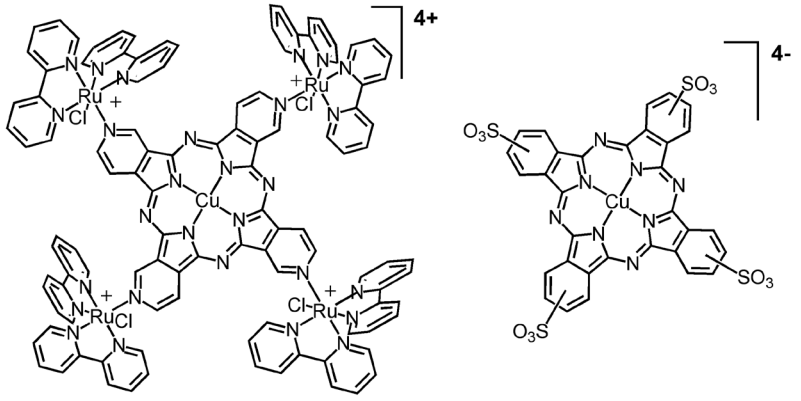

Figure 1. Structural representation of tetraruthenated copper(II)-tetra(3,4-pyridyl) porphyrazine, and tetrasulfonated copper(II)-phthalocyanine used for the preparation of layer-by-layer electrostatic assembled films.

N,N'-dimethylformamide (DMF), using a Princeton Applied Research model 283 potentiostat. A conventional three electrode cell consisting of a platinum disk working electrode, Ag/Ag^+ (0.010 mol dm^{-3}, in acetonitrile, E^o = 0.503 V *vs.* SHE) reference electrode, and a coiled platinum wire auxiliary electrode was employed. The solvents were HPLC grade, but DMF was dried over anhydrous $CuSO_4$ and distilled under vacuum immediately before use. The electrolyte salt $[(C_2H_5)_4N]ClO_4$, or $TEAClO_4$, was purified by recrystallization in water and dried under vacuum. The spectroelectrochemistry data were collected using a previously described homemade thin-layer cell and a PAR model 173 potentiostat/galvanostat in parallel with the HP-8453A spectrophotometer.[37] Electrochemical impedance spectroscopy measurements were carried out with an AUTOLAB PGSTAT30 equipment and a conventional three electrodes electrochemical cell, in the 1 to 10^5 Hz range. Electrospray mass spectra were recorded for the samples dissolved in pure methanol, using a Q-Tof (Micromass) mass spectrometer with a quadrupole (Qq) and high-resolution orthogonal time of flight (o-TOF) configuration.

Results and Discussion

The chemical constitution of the tetraruthenated porphyrazines was confirmed by means of electrospray mass spectrometry. The observed fragmentation pattern can be seen in the global scheme shown in the Figure 2. The $[CuTRPyPz]^{4+}$ species exhibits the molecular ion peak $[C_{108}H_{74}N_{28}CuRu_4Cl_4]^{4+}$ (MM = 2374 g mol^{-1}) at *m/z* 594 and Δ(*m/z*) 0.25, in the free form, but it also appears as an ion pair, associated with the TFMS ion, at *m/z* 841 (Δ(*m/z*) 0.33). In the gas phase, the tetraruthenated species is more susceptible to the electrostatic repulsion between the positively charged $[Ru(bpy)_2Cl]^+$ groups,[28,38,39] undergoing a sequential dissociation of the peripheral complexes. This process generates either the $[Ru(bpy)_2Cl]^+$ species at *m/z* 449, or the solvated $[Ru(bpy)_2(CH_3OH)Cl]^+$ ones at *m/z* 481, as well as the corresponding fragments containing the porphyrazine ring. Doubly and triply charged pyridylporphyrazine bound to two or three $[Ru(bpy)_2Cl]^+$ complexes have been detected by the characteristic peaks at *m/z* 642 and *m/z* 738. The monosubstituted species resulting from the loss of three peripheral ruthenium complexes has been observed at *m/z* 1027.

Electrochemistry and spectroelectrochemistry

The cyclic voltammograms of $[CuTRPyPz]^{4+}$ exhibit a series of electrochemical waves displaying 1:1 and 1:4 relative intensities, in the –1.5 to 1.7 V range, as shown in Figure 3. The strong waves at 0.97 V are characteristic of the reversible Ru(III/II) redox couple (wave A).

The spectra of the $[CuTRPyPz]^{4+}$ species in methanol, ethanol or DMF solutions exhibit a complex absorption profile, which can be deconvoluted in terms of a series of bands at 296, 326, 356, 382, 430, 490, 602 and 702 nm, as shown in Figure 4. By comparison with the electronic spectra of similar species,[34] the peaks at 296, 326 and 490 nm can be assigned, respectively, as internal $\pi\rightarrow\pi^*$ transitions of the bipyridyl ligands, and as $Ru^{II}\rightarrow$bpy ($d\pi\rightarrow p\pi_2^*$) and ($d\pi\rightarrow p\pi_1^*$) metal-ligand charge transfer transitions (MLCT) in the $[Ru(bpy)_2Cl]^+$ group. The bands at 356, 382 nm can be ascribed to the B_2 and B_1 Soret bands, and those at 602, 702 nm to the Q(0,1) and Q(0,0) bands of CuTPyPz. The 430 nm is consistent with the MLCT $Ru^{II}\rightarrow$TPyPz ($d\pi\rightarrow p\pi^*$) transition.

The porphyrazine Q bands at 602 and 702 nm exhibit are relatively broad, reflecting the exciton coupling associated with the formation of π–stacked species.[40]

The corresponding spectroelectrochemical results are shown in Figure 5. The oxidation of the peripheral complexes at 0.97 V led to the disappearance of the MLCT band at 490 nm, while the broad Q bands at 602 and 706 nm collapsed into a narrow structured band at 670 nm (Figure 5A), characteristic of non associated species. This is an interesting result which can be explained considering that the oxidation of the peripheral Ru(II) complexes to Ru(III), increases the positive charge on the tetraruthenated species, from +4 to +8, lowering the probability of occurring π-stacking interactions. At 1.5 V, a weak, irreversible wave was also detected, suggesting the oxidation of the porphyrazine ring. Unfortunately, spectroelectrochemical measurements at this potential were precluded by the decomposition of the complex.

Four successive reduction reactions were observed in the range of 0.5 to –1.1 V. According to the corresponding spectroelectrochemical patterns (Figure 5B-E) one can conclude that they do not involve the peripheral ruthenium complexes, since the bipyridyl $\pi\rightarrow\pi^*$ band at 293 nm and the metal-ligand charge transfer band at 490 nm remained practically unchanged.

The quasi-reversible processes at –0.11 and –0.50 V (waves B and C) were ascribed to the first and second monoelectronic reductions of the porphyrazine ring. As a matter of fact, when the potential was changed from 0.50 to –0.20 V, a decrease in the intensity of the Soret and Q bands at 360 and 710 nm, and an increase of the absorbance at 550 nm were observed, corresponding to the formation of the porphyrazine radical anion species. When the potentials were changed from –0.20 to –0.60 V, the intensity

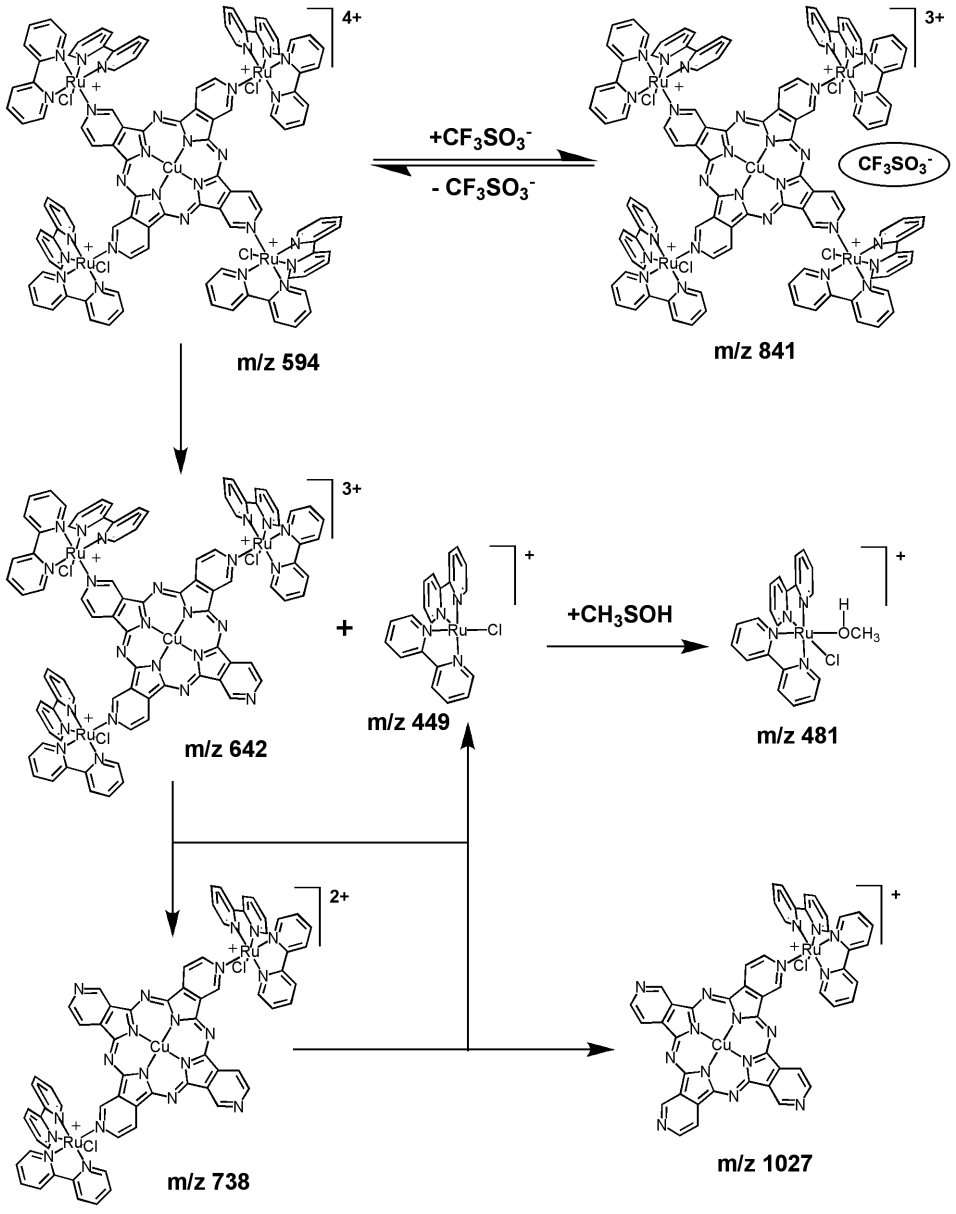

Figure 2. ESI-MS dissociation pattern for the $[CuTRuPyPz]^{4+}$ complex.

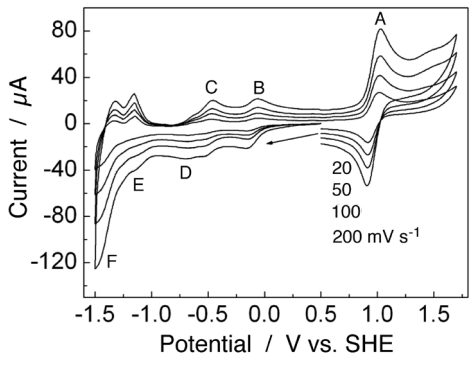

Figure 3. Cyclic voltammograms of the 2.8×10^{-3} mol dm^{-3} $[CuTRPyPz]^{4+}$ in DMF solution containing 0.10 mol dm^{-3} of $TEAClO_4$ in 1.7 to –1.5 V range, on Pt-disk electrode.

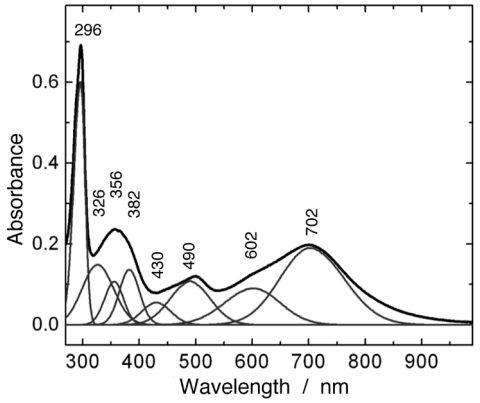

Figure 4. UV-Vis spectrum of 3.4×10^{-6} mol dm^{-3} solution of $[CuTRPyPz]^{4+}$ in methanol.

of the bands attributed to the radical anion decreased and simultaneously a new band rose at 853 nm, consistent with the formation of the porphyrazine dianion.

The third reduction process (wave D) observed in the –0.60 to –0.80 V range, led to the decay of the 853 nm band, and to the increase of absorbance at 525 nm, giving rise to a broad envelope. The fourth reduction process was found in the –0.80 to –1.20 V range. In this case, a very broad band appeared at 823 nm concomitantly with the decrease of the band at 525 nm. These waves are centered at the reduced copper-macrocyclic ring. Considering the previous reduction of the porphyrazine center, the participation of Cu(I) and Cu(0) states in the two processes seems very probable.

The last wave, at −1.39 V, exhibits an intensity comparable to that of the Ru(III/II) process, leading to pronounced changes in the $[Ru(bpy)_2Cl]^+$ bands at 293 and 490 nm, supporting the reduction of the bipyridine ligand. The expected 4:1 intensity ratio between the ruthenium complexes and porphyrazine centered electrochemical processes has been observed, and also confirmed by differential pulse voltammetry (DPV) (not shown).

Preparation and electrochemical properties of the supramolecular films

Tetraruthenated porphyrins and porphyrazines are known to form stable and adherent films on electrodes or substrates like indium tin oxide (ITO) or glassy carbon.[33,36,41-43] Such molecular films are relatively soluble in conventional solvents, but can be employed in aqueous solution in the presence of a large excess of counter ions, such as PF_6^-, triflate or perchlorate anions, in order to reduce their solubility. A better approach, however, is by carrying out a layer-by-layer self-assembly, based on a combination with sulphonated porphyrins or phtalocyanines. As a matter of fact, we have observed that the tetraruthenated porphyrazines form highly homogeneous and stable films by electrostatic self-assembly with tetrasulfonated copper(II) phthalocyanines (Figure 1). The build-up of such $[CuTRuPyPz]^{4+}/[CuTSPc]^{4-}$ electrostatic assembled bilayered films on ITO can be monitored spectrophotometrically, as shown in Figure 6. There is a steady increase of the absorption bands (inset Figure 6) associated with the ruthenium complexes and the copper(II) porphyrazine and phtalocyanine, as expected for the deposition of equivalent amounts of each species, at each diping process.

In order to investigate the conduction and electrocatalytic properties of the $[CuTRuPyPz]^{4+}/[CuTSPc]^{4-}$ films, glassy carbon rotating disk electrodes were used, as shown in Figure 7. The layer-by-layer films exhibited a couple of reversible sine-shaped waves at 0.97 V related to the oxidation of the peripheral ruthenium ions, *i. e.* [Ru(II)→Ru(III)]. This electrochemical process is

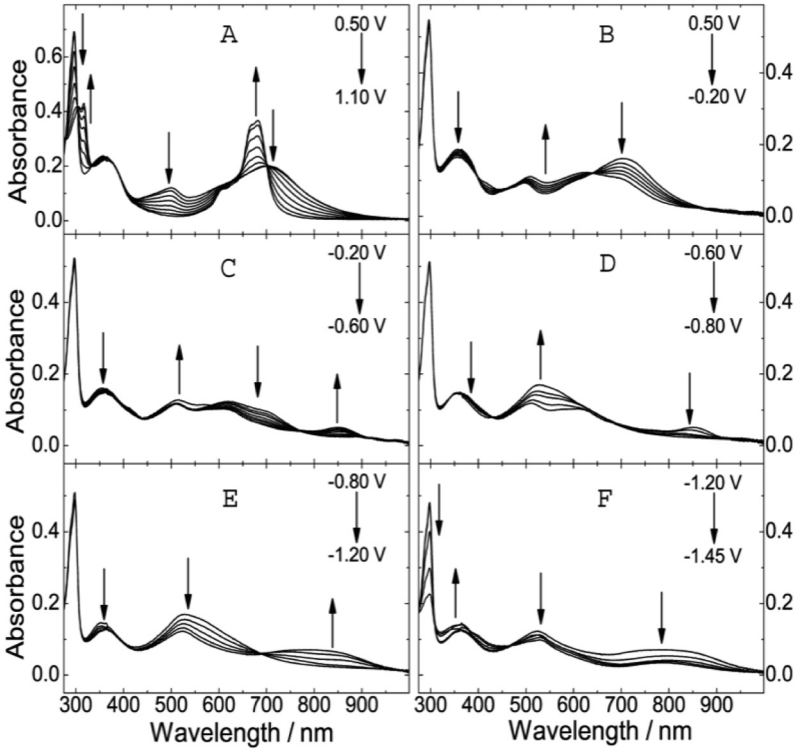

Figure 5. UV-Vis spectroelectrochemistry of a $[CuTRPyPz]^{4+}$ 0.10 mmol dm^{-3} in DMF solution containing 0.10 mol dm^{-3} of $TEAClO_4$ in –1.45 to 1.1 V range.

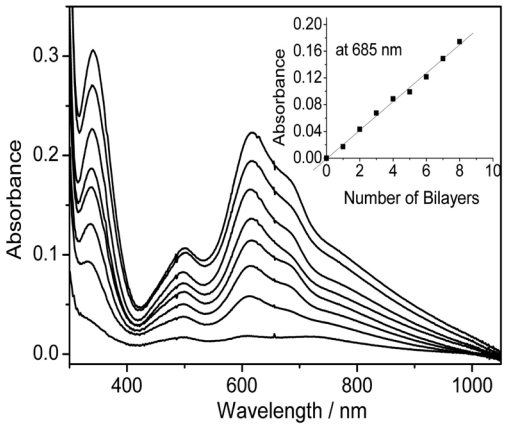

Figure 6. Build-up of layer-by-layer $[CuTRuPyPz]^{4+}/[CuTSPc]^{4-}$ films onto ITO glass, monitored by UV-Vis spectroscopy. Inset: plot of absorbance at 685 nm *vs.* the number of bilayers.

reversible, exhibiting a peak current linearly dependent on the scan rate, as expected when the redox centers are immobilized on the electrode surface.

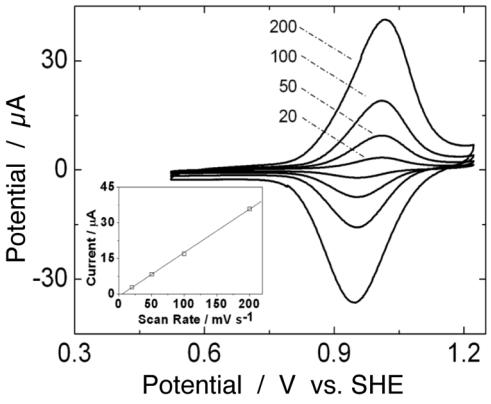

Figure 7. Cyclic voltammograms of a modified glassy carbon electrode containing three $[CuTRuPyPz]^{4+}/[CuTSPc]^{4-}$ bilayers, surface coverage $\Gamma = 1.86 \times 10^{-10}$ mol cm^{-2} in 0.5 mol dm^{-3} $NaNO_3$, pH 4.5 aqueous solution. Inset: plot of the peak current intensities as a function of the scan rate.

The conduction properties of the $[CuTRuPyPz]^{4+}/[CuTSPc]^{4-}$ films were investigated by means of impedance spectroscopy. The Nyquist plots of the data collected at 0.72 V and 0.97 V for $\Gamma = 1.86 \times 10^{-10}$ mol cm^{-2} are shown in Figure 8. At 0.72 V, there is no significant redox process. In this case, the beginning of a semi-circle can be observed in the high-frequency region, followed by a very short diffusion controlled region and saturation at lower frequencies (inset Figure 8). This kind of response can be analyzed using a simple Randles RC circuit, from which a charge-transfer resistance, R_{CT} *ca.* 60 Ω can be evaluated. The spectrum profile and the R_{CT} value are similar to those obtained for analogous free-base tetraruthenated porphyrazine.[33] On the other hand, the Nyquist plot obtained at 0.97 V, *i.e.*, at Ru(III/II) redox potential exhibited a quite different profile as compared with the free-base derivative, in which case an inductive component has been reported.[33] In the case of the copper(II) derivative no semi-circle associated with activated electron transfer processes nor diffusion controlled Warburg region could be observed, but only a saturation line indicated by a curve nearly perpendicular to the Z_{Re} axis. This indicates that at this potential, the electrode/film/solution interface behaves as a low resistance metallic electronic conductor. Accordingly, the electron hopping between the ruthenium centers should be very fast, at applied potentials near the $E_{1/2}$ of the Ru(III/II) redox pair.

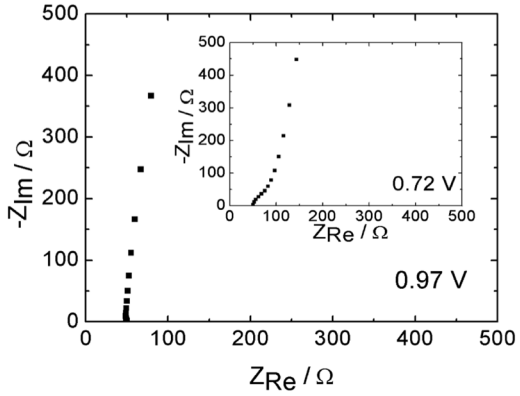

Figure 8. Nyquist plots of the impedance spectroscopy data obtained for a glassy carbon electrode modified with $[CuTRuPyPz]^{4+}/[CuTSPc]^{4-}$ film ($\Gamma = 1.86 \times 10^{-10}$ mol cm^{-2}) in 0.5 mol dm^{-3} $NaNO_3$, pH 4.5 aqueous solution, frequencies ranging from 1 Hz to 100 kHz, at 0.97 V and 0.72 V (inset).

Electrocatalytic properties of the layer-by-layer films

Although nitrite and sulfite ions exhibit detectable eletrochemical response in most conventional bare electrodes, the processes are usually irreproducible and severely complicated by electrode poisoning effects. In contrast, when nitrite and sulphite ions are added into the buffered electrolyte solution (Figure 9), the anodic wave at 1.1 V in the $[CuTRuPyPz]^{4+}/[CuTSPc]^{4-}$ films exhibits a large intensification, which increases as a function of the concentration of those species, with no evidence for the corresponding cathodic wave. This observation is consistent with a relatively fast heterogeneous charge-transfer process mediated by the Ru(III)/(II) sites, which act as conduction gates, generating an electric rectifying response.

The kinetics of the nitrite to nitrate mediated oxidation reaction were studied by RDE voltammetry in the 100-4000 rpm rotation range. Typical current *vs.* potential curves are shown in Figure 10 A. The voltammograms exhibited a typical sigmoidal shaped profile at low frequencies and concentrations, reaching the limiting currents

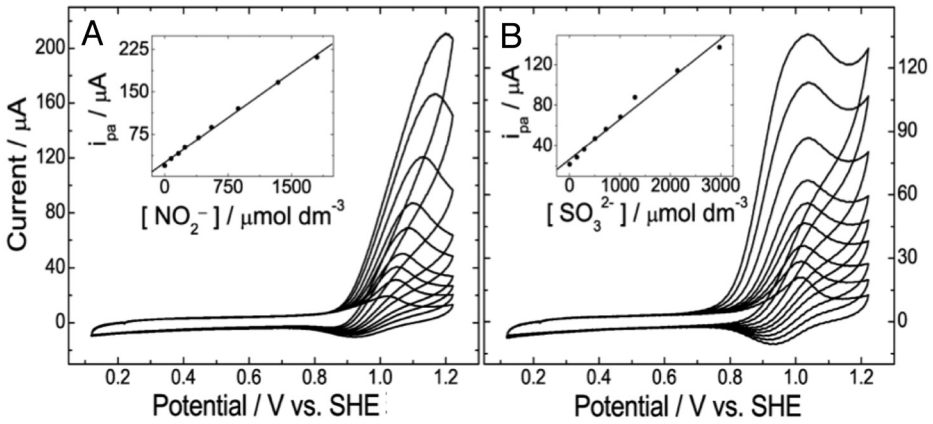

Figure 9. Cyclic voltammograms of glassy carbon electrodes modified with layer-by-layer electrostatic assembled films of $[CuTRuPyPz]^{4+}/[CuTSPc]^{4-}$, (A) $\Gamma = 0.5$ nmol cm^{-2} and (B) $\Gamma = 0.4$ nmol cm^{-2}; in the presence of increasing concentration of (A) $NaNO_2$ and (B) Na_2SO_3 (0.05 to 3 mmol dm^{-3} range), in phosphate buffer pH 6.8, [KNO_3] = 0.5 mol dm^{-3}. Inset: Plot of i_{pacat} *vs.* substrate concentration.

at 1.1 V. However, for the determination of the constants, a kinetically limited condition is required. For this reason, the concentration of the substrate was increased up to the point where the Levich plot exhibited a small but increasing curvature as a function of the rotation rate. This is a clear indication that the current is no longer limited by diffusion, but also by the kinetic of the heterogeneous electron-transfer reaction at the film/electrode interface; more specifically, by the reaction between the electrochemically generated mediator (Ru(III)) and the substrate (NO_2^-) in solution. The parameter $\Gamma k_f = 1.45 \times 10^{-2}$ cm s^{-1} ($\Gamma = 1.86 \times 10^{-10}$ mol cm^{-2}) was calculated from the linear coefficient of the Koutecky-Levich plots (Figure 10 B) as a function of the NO_2^- concentration (Figure 10 C).

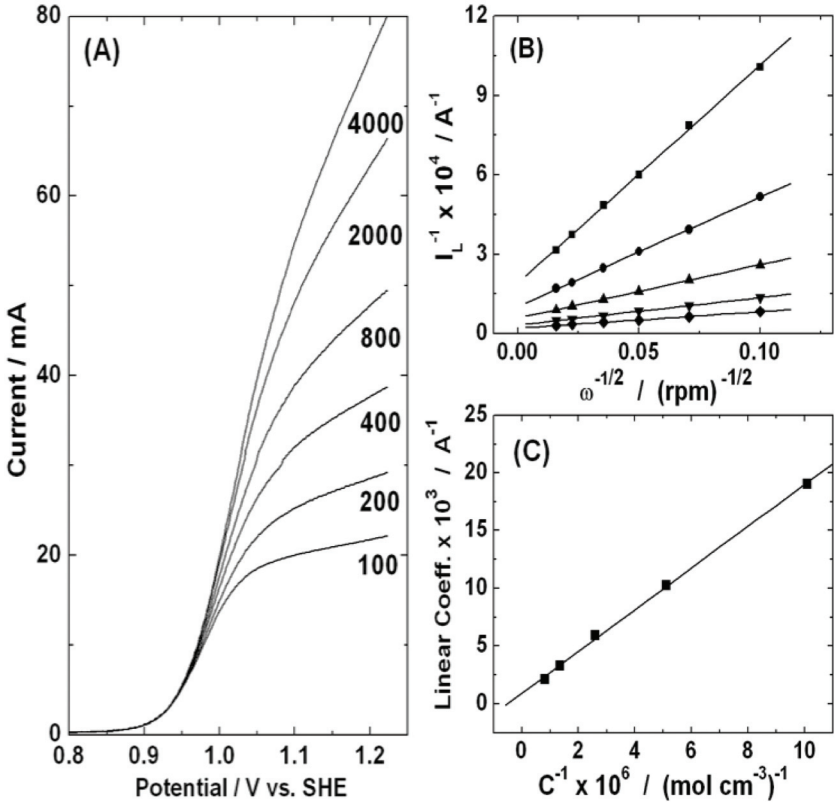

Figure 10. (A) RDE voltammograms of a GC electrode modified with electrostatic assembled films of $[CuTRuPyPz]^{4+}/[CuTSPc]^{4-}$ ($\Gamma = 1.86 \times 10^{-10}$ mol cm^{-2}) in 1.96×10^{-3} mol dm^{-3} $NaNO_2$ solution, $NaNO_3$ 0.5 mol dm^{-3} M, pH 4.5 (acetate buffer), $100 < \nu < 4000$ rpm. (B) Koutecky-Levich plot for RDE experiments using increasing concentrations of nitrite: 0.99 (square), 1.96 (circle), 3.85 (up triangle), 7.41 (down triangle), and 12.3×10^{-4} mol dm^{-3} (diamond). The limiting catalytic current was measured at 1.1 V; (C) Plot of linear coefficients of Koutecky-Levich plots *vs.* reciprocal of nitrite concentration.

Unfortunately, in the case of the sulfite ions, the kinetics of oxidation mediated by the $[CuTRuPyPz]^{4+}$/$[CuTSPc]^{4-}$ film were too fast to be monitored by RDE, such that the Levich plot was essentially linear up to a concentration of about 10 mmol dm^{-3} of the substrate, and rotation rate of 5000 rpm.

The RDE experiments were also carried out by varying the thickness of the molecular mediator, in order to evaluate the contribution of the surface concentration of the electrocatalytic active sites in the film, and to determine the value of k_f. Unfortunately, at high surface concentrations, the film resulted too rough, leading to a large dispersion of the $k_f\Gamma$ results. On the other hand, at very low Γ, one increases the chances that the electrode surface is not completely covered. For this reason, we selected the intermediate data corresponding to $1.5 \times 10^{-10} < \Gamma$ / mol $cm^{-2} < 1.5 \times 10^{-9}$ for the determination of k_f from the slope of $k_f\Gamma$ *vs.* $[NO_2^-]$ plot. As a matter of fact, a linear plot has been obtained, yielding a rate constant $k_f = 3.3 \times 10^4$ mol dm^{-3} s^{-1}. This value is about 10 times higher than that previously obtained for the for self-assembled films based on tetraruthenated cobalt-porphyrin and tetrasulphonated zinc-porphyrin, and it is comparable to the best results yet reported for the films of electropolymerized porphyrins coordinated to four $[Ru(5\text{-}ClPhen)_2Cl]^+$ complexes.[44,45]

Conclusions

The tetraruthenated copper(II)-tetra(3,4-pyridyl) porphyrazine species provides a versatile π-conjugated system, contrasting with the related *meso*-tetra-pyridylporphyrin analogues by exhibiting strong electronic interaction between the coordinated peripheral complexes and the central ring. The spectrometric, spectroscopic and electrochemical data are in complete agreement with the proposed composition. Electrospray mass experiments revealed an ion-pairing process in the gas phase, and the occurrence of a sequential fragmentation of the peripheral complexes. Layer-by-layer (lbl) electrostatic assembled films were successfully generated by the appropriate combination of $[CuTRuPyPz]^{4+}$ with copper(II)-tetrasulfonated phtalocyanine, exhibiting metallic conductivity near the Ru(III/II) redox potential, as well as enhanced electrocatalytic activity for oxidation of nitrite and sulfite ions.

Acknowledgments

The authors would like to thank the Fundação de Amparo à Pesquisa do Estado de São Paulo (FAPESP), Conselho Nacional de Desenvolvimento Científico e Tecnológico (CNPq), and Instituto do Milênio de Materiais Complexos (IMMC) for financial support, and Dr. D. M. Tomazela for her precious help in the mass spectrometry measurements.

References

1. Kobayashi, N.; *Coord. Chem. Rev.* **2002**, *227*, 129.
2. Kobayashi, N.; *Coord. Chem. Rev.* **2001**, *219*, 99.
3. Rodriguez-Morgade, M. S.; Stuzhin, P. A.; *J. Porphyrins Phthalocyanines* **2004**, *8*, 1129.
4. Salabert, I.; Tranthi, T. H.; Ali, H.; Vanlier, J.; Houde, D.; Keszei, E.; *Chem. Phys. Lett.* **1994**, *223*, 313.
5. vanNostrum, C. F.; Nolte, R. J. M.; *Chem. Commun.* **1996**, *21*, 2385.
6. Ambroise, A.; Wagner, R. W.; Rao, P. D.; Riggs, J. A.; Hascoat, P.; Diers, J. R.; Seth, J.; Lammi, R. K.; Bocian, D. F.; Holten, D.; Lindsey, J. S.; *Chem. Mater.* **2001**, *13*, 1023.
7. Velazquez, C. S.; Fox, G. A.; Broderick, W. E.; Andersen, K. A.; Anderson, O. P.; Barrett, A. G. M.; Hoffman, B. M.; *J. Am. Chem. Soc.* **1992**, *114*, 7416.
8. Li, X. Y.; Ng, D. K. P.; *Eur. J. Inorg. Chem.* **2000**, 1845.
9. Kobayashi, N.; Nakajima, S.; Osa, T.; *Chem. Lett.* **1992**, 2415.
10. Ou, Z. P.; E, W; Shao, J. G.; Burn, P. L.; Sheehan, C. S.; Walton, R.; Kadish, K. M.; Crossley, M. J.; *J. Porphyrins Phthalocyanines* **2005**, *9*, 142.
11. Zenkevich, E. I.; von Borczyskowski, C.; Shulga, A. M.; *J. Porphyrins Phthalocyanines* **2003**, *7*, 731.
12. Spasojevic, I.; Batinic-Haberle, I.; *Inorg. Chim. Acta* **2001**, *317*, 230.
13. Jiang, J. Z.; Liu, W.; Law, W. F.; Ng, D. K. P.; *Inorg. Chim. Acta* **1998**, *268*, 49.
14. Love, J. C.; Estroff, L. A.; Kriebel, J. K.; Nuzzo, R. G.; Whitesides, G. M.; *Chem. Rev.* **2005**, *105*, 1103.
15. Shen, Z. Y.; Yan, H.; Wang, T.; Seeman, N. C.; *J. Am. Chem. Soc.* **2004**, *126*, 1666.
16. Szleifer, I.; Yerushalmi-Rozen, R.; *Polymer* **2005**, *46*, 7803.
17. Chau, R.; Brask, J.; Datta, S.; Dewey, G.; Doczy, M.; Doyle, B.; Kavalieros, J.; Jin, B.; Metz, M.; Majumdar, A.; Radosavljevic, M.; *Microelectron. Eng.* **2005**, *80*, 1.
18. Toma, H. E.; *J. Braz. Chem. Soc*. **2003**, *14*, 845.
19. Toma, H. E.; *Current Science* **2008**, *95*, 1202.
20. Manna, J.; Kuehl, C. J.; Whiteford, J. A.; Stang, P. J.; *Organometallics* **1997**, *16*, 1897.
21. Drain, C. M.; Goldberg, I.; Sylvain, I.; Falber, A. In *Functional Molecular Nanostructures*; Schlüter, A. D., ed.; *Topics Curr. Chem.* **2005**, *248*, 55.
22. Hofmeier, H.; Andres, P. R.; Hoogenboom, R.; Herdtweck, E.; Schubert, U. S.; *Austr. J. Chem.* **2004**, *57*, 419.
23. Milic, T. N.; Chi, N.; Yablon, D. G.; Flynn, G. W.; Batteas, J. D.; Drain, C. M.; *Angew. Chem., Int. Ed*. **2002**, *41*, 2117.

24. Drain, C. M.; Batteas, J. D.; Flynn, G. W.; Milic, T.; Chi, N.; Yablon, D. G.; Sommers, H.; *Proc. Natl. Acad. Sci. U. S. A.* **2002**, *99*, 6498.
25. Zimmer, A.; Muller, I.; Reiss, G. J.; Caneschi, A.; Gatteschi, D.; Hegetschweiler, K.; *Eur. J. Inorg. Chem.* **1998**, 2079.
26. Alessio, E.; Macchi, M.; Heath, S. L.; Marzilli, L. G.; *Inorg. Chem.* **1997**, *36*, 5614.
27. Nunes, G. S.; Mayer, I.; Toma, H. E.; Araki, K.; *J. Catal.* **2005**, *236*, 55.
28. Mayer, I.; Eberlin, M. N.; Tomazela, D. M.; Toma, H. E.; Araki, K.; *J. Braz. Chem. Soc.* **2005**, *16*, 418.
29. Araki, K.; Winnischofer, H.; Viana, H. E. B.; Toyama, M. M.; Engelmann, F. M.; Mayer, I.; Formiga, A. L. B.; Toma, H. E.; *J. Electroanal. Chem.* **2004**, *562*, 145.
30. Dovidauskas, S.; Toma, H. E.; Araki, K.; Sacco, H. C.; Iamamoto, Y.; *Inorg. Chim. Acta* **2000**, *305*, 206.
31. Winnischofer, H.; Otake, V. Y.; Dovidauskas, S.; Nakamura, M.; Toma, H. E.; Araki, K.; *Electrochim. Acta* **2004**, *49*, 3711.
32. Mayer, I.; G. S. Nunes, Toma, H. E.; Araki, K.; *Eur. J. Inorg. Chem.* **2005**, 850.
33. Toyama, M. M.; Demets, G. J. F.; Araki, K.; Toma, H. E.; *Electrochem. Commun.* **2000**, *2*, 749.
34. Toyama, M. M.; Franco, M.; Catalani, L. H.; Araki, K.; Toma, H. E.; *J. Photochem. Photobiol., A* **1998**, *118*, 11.
35. Toma, H. E.; Araki, K.; *Coord. Chem. Rev.* **2000**, *196*, 307.
36. Araki, K.; Wagner, M. J.; Wringhton, M. S.; *Langmuir* **1996**, *12*, 5393.
37. Toma, H. E.; Araki, K.; *Curr. Org. Chem.* **2002**, *6*, 21.
38. Tomazela, D. M.; Gozzo, F. C.; Mayer, I.; Engelmann, F. M.; Araki, K.; Toma, H. E.; Eberlin, M. N.; *J. Mass Spectrom.* **2004**, *39*, 1161.
39. Mayer, I.; Formiga, A. L. B.; Engelmann, F. M.; Winnischofer, H.; Oliveira, P. V.; Tomazela, D. M.; Eberlin, M. N.; Toma, H. E.; Araki, K.; *Inorg. Chim. Acta* **2005**, *358*, 2629.
40. Dodsworth, E. S.; Lever, A. B. P.; Seymour, P.; Leznoff, C. C.; *J. Phys. Chem.* **1985**, *89*, 5698.
41. AAAraki, K.; Toma, H. E.; *Electrochim. Acta* **1999**, *44*, 1577.
42. Araki, K.; Angnes, L.; Toma, H. E.; *Adv. Mater.* **1995**, *7*, 554.
43. Azevedo, C. M. N.; Araki, K.; Angnes, L.; Toma, H. E.; *Electroanalysis* **1998**, *10*, 467.
44. da Rocha, J. R. C.; Demets, G. J. F.; Bertotti, M.; Araki, K.; Toma, H. E.; *J. Electroanal. Chem.* **2002**, *526*, 69.
45. Winnischofer, H.; Lima, S. S.; Araki, K.; Toma, H. E.; *Anal. Chim. Acta* **2003**, *480*, 97.

Received: December 7, 2008
Web Release Date: April 30, 2009

FAPESP helped in meeting the publication costs of this article.